Intra-fraction motion monitoring during fast modulated radiotherapy delivery in a closed-bore gantry linac

Laurence Delombaerde [a,b,*], Saskia Petillion [b], Caroline Weltens [a,b], Tom Depuydt [a,b,*]

[a] Department of Oncology, KU Leuven, Herestraat 49, Leuven 3000, Belgium
[b] Department of Radiation Oncology, University Hospitals Leuven, Herestraat 49, Leuven 3000, Belgium

ARTICLE INFO

ABSTRACT

Background and purpose: New closed-bore linacs allow for highly streamlined workflows and fast treatment delivery resulting in brief treatment sessions. Motion management technology has only recently been integrated inside the bore, yet is required in future online adaptive workflows. We measured patient motion during every step of the workflow: image acquisition, evaluation and treatment delivery using surface scanning.

Materials and methods: Nineteen patients treated for breast, lung or esophageal cancer were prospectively monitored from the end of setup to the end of treatment delivery in the Halcyon linac (Varian Medical Systems). Motion of the chest was tracked by way of 6 degrees-of-freedom surface tracking. Baseline drift and rate of drift were determined. The influence of fraction number, patient and fraction duration were analyzed with multi-way ANOVA.

Results: Median fraction duration was 4 min 48 s including the IGRT procedure (kV-CBCT acquisition and evaluation) (N = 221). Baseline drift at the end of the fraction was -1.8 ± 1.5 mm in the anterior-posterior, -0.0 ± 1.7 mm in the cranio-caudal direction and 0.1 ± 1.8 mm in the medio-lateral direction of which 75% occurred during the IGRT procedure. The highest rate of baseline drift was observed between 1 and 2 min after the end of patient setup (-0.62 mm/min). Baseline drift was patient and fraction duration dependent (p < 0.001), but fraction number was not significant (p = 0.33).

Conclusion: Even during short treatment sessions, patient baseline drift is not negligible. Drift is largest during the initial minutes after completion of patient setup, during verification imaging and evaluation. Patients will need to be monitored during extended contouring and re-planning procedures in online adaptive workflows.

1. Introduction

Modern radiotherapy techniques enable delivery of highly complex dose distributions with maximal dose to the target to achieve tumor control, while minimizing the dose to healthy tissues to limit early and late side effects, where an accurate reproduction of the patients' posture as determined on the simulation CT is required during every fraction. Inter-fraction variability in target position and patient setup is accounted for in the use of a safety margin. Generally setup verification images are analyzed for systematic and random inter fraction errors from which, with an appropriate margin recipe such as Van Herk's formula [1], the clinical-to-planning target (CTV-to-PTV) margin is calculated. This approach however does not take into account intra fraction motion such as baseline drift where the patient relaxes and gradually deviates from their original position. The magnitude and orientation of baseline drift has been extensively studied for a range of sites such as lung and liver tumors with radiopaque markers [2,3,4,5], breast cancer patients with a laser system [6] or optical surface scanning system [7] and general chest motion using a marker block system [8]. Previous studies have focused on fractions exceeding 20 to 30 min such as lung Stereotactic Body Radiotherapy (SBRT) treatments [3], TomoTherapy deliveries [9] or Accelerated Partial Breast Irradiations (APBI) [10]. Both Ricotti et al. [9] and Wiant et al. [11] note that breast cancer patients reach a stable position after 6–8 min. Yet, improvements in on-board imaging equipment and treatment delivery technology have resulted in decreased fraction durations, during which a stable position might not be reached.

In 2017 a fast-rotating closed-bored linac with a simplified and streamlined workflow was released. Cone-beam CT (CBCT) verification imaging can be acquired in 17 s and the increased gantry rotation and

* Corresponding authors at: Department of Oncology, KU Leuven, Herestraat 49, Leuven 3000, Belgium (T. Depuydt).
E-mail addresses: laurence.delombaerde@uzleuven.be (L. Delombaerde), tom.depuydt@uzleuven.be (T. Depuydt).

leaf speed allow for a faster volumetric modulated arc radiotherapy (VMAT) or intensity modulated radiotherapy (IMRT) delivery with similar plan quality compared to C-arm linacs for a range of indications [12–14]. Due to limited access to the patient by the radiotherapy technologists (RTT) inside the bore, patient setup is performed in front of the linac after which the couch automatically translates to the treatment isocenter. Setup can be performed either guided by the built-in lasers or using a surface scanning system [15,16], however after translation to the treatment isocenter, the patient falls outside the reach of the ceiling-mounted surface monitoring systems [17,18]. To investigate the potential added value, we have developed an intra-bore surface scanning system to monitor patient motion during treatment [16,19] to be able to assess motion during the image guidance (IGRT) procedures (e.g. kV-CBCT acquisition and evaluation) and treatment delivery. In 2020 the first commercial system for intra-bore monitoring was released which has been commissioned by Nguyen et al. [20]. The authors were also the first to report on intra-fraction motion of breast cancer patients treated on the closed-bore linac [21].

In this study we aim to quantify patient motion inside the fast closed-bore linac using a compact intra-bore surface scanning system. As volumetric verification imaging is becoming closer to a 'snapshot' of the patients' position due to the increased efficiency of acquisition, motion during image evaluation becomes an important factor in treatment delivery accuracy. We therefore monitored patients during every step of a fraction – imaging, online image verification and treatment delivery – to assess the relative contribution.

2. Materials and methods

2.1. Patient data

Nineteen patients were prospectively included in this clinical study, approved by the Internal Review Board, after giving informed consent. The included population were patients treated in the thoracic region (breast, esophageal and lung cancer patients) on a Halcyon linac (Varian Medical Systems). Of the 19 patients in this study, 9 were breast cancer patients (9/9 female), 6 were lung cancer patients (1/6 female) and 4 were esophageal cancer patients (1/4 female).

2.2. Treatment workflow

Patients were treated on a Varian Halcyon where initial positioning is performed in front of the bore at the setup isocenter. All patients were positioned with the arms up, with the aid of a chest board (Posirest™, Civco) and a knee support (Kneefix™, Civco). A foam mattress was used to improve patient comfort. All breast cancer patients were setup using AlignRT (v5.1 and v6.2, VisionRT Ltd.) using a tolerance of 3 mm and 1.5° from the planned position. Esophageal and lung cancer patients were setup using skin marks and the Halcyon lasers. After translation to the treatment isocenter, a kV-CBCT was acquired every fraction using either the breast or thorax protocol (acquisition time 17 s or 30 s resp.). Online 3D registration to the planning CT was performed guided by our in-house "traffic-light" IGRT protocol for each indication. RTTs evaluate if a set of predefined OAR and target volumes are confined within the CT contours, e.g. for lung carcinomas the tumor should be within the tumor planning target volume (PTV), for breast cancer swelling is assessed using an expansion margin. All corrections were applied for every fraction. Couch motion is limited to translations only. These steps – image acquisition and evaluation – are denoted *IGRT procedure* from hereon. Breast cancer patients were then treated using a dual partial arc VMAT protocol with 2.66 Gy to the tumor bed and 2.17 Gy to the whole breast for 21 fractions. Esophageal cancer patients were treated with a 7-field IMRT and lung patients with a 9-field IMRT class solution where the dose prescription varied (e.g. 20×2.75 Gy, 33×2 Gy) depending on tumor staging, cell type and/or use of concomitant chemotherapy. Total treatment delivery time ranged from 1 min and 5 s to 3 min and 19 s

from the start of the first field to the end of the last field. The total time patients spent on the couch at the treatment isocenter was median of 4 min 48 s (range 2 min 50–10 min 35 s) where 99% of all fractions were completed within 8 min. The time until the online matching correction was applied was median 2 min 50 s, where the time required for image acquisition and evaluation constituted 60% of the total time the patient spent on the couch.

2.3. Surface scanning acquisition

An intra-bore surface scanning system monitored the patient from completion of the setup (so after translation of the couch to the treatment isocenter) until the end of radiation delivery. Monitoring was initiated within two seconds after execution of the couch shift. This surface scanning system is described in detail in Delombaerde et al. [16,19] but the basics are reiterated here. The system consists of two Kinect™ for Windows cameras (Microsoft, Redmond, VA, USA) mounted at the back of the Halcyon bore to image the patient while at the treatment isocenter. The cameras use structured-light technology to acquire depth information from which the patient's body surface is reconstructed at 4 Hz. Every fraction, a region-of-interest (ROI) consisting of the breast for breast cancer patients or chest for lung and esophageal cancer patients was delineated on the first reconstructed surface after completion of setup, which is then tracked by way of an Iterative Closest Point (ICP) 6 degrees-of-freedom (DoF) rigid registration providing a continuous signal of intra fraction motion. A total of 221 complete fractions were available for analysis with a median of 13 fractions per patient (range 4–16).

2.4. Data analysis

The original signal acquired with surface imaging consists of a low-frequency component – baseline drift – and a high frequency component – cyclic breathing. To extract the total baseline drift of the patient during the entire fraction, the signal was manually corrected after the couch shift, performed after imaging, as shown in Fig. 1. The cyclic breathing was averaged out by use of a moving mean filter with a 60 s interval. The contribution of drift during image acquisition and evaluation relative to the total drift was determined. The peak-to-peak breathing amplitude was extracted from the original signal by calculating the amplitude between the extreme inhale and exhale signal, averaged over four
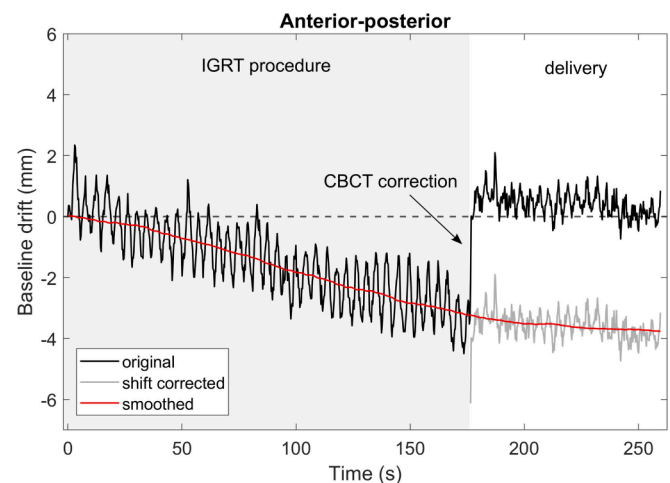
Fig. 1. The original surface scanning signal (only the AP direction is shown, negative values indicate a drift in the posterior direction) is manually corrected after the couch shift to extract the total baseline drift of the patient. A moving mean filter is applied to remove the cyclic breathing. This VMAT-SIB breast treatment was completed in 260 s including volumetric imaging, evaluation and delivery.

breathing cycles. This amplitude was compared to the total baseline drift for all patients. The rate of baseline drift was calculated in 60 s intervals both for all patients and per indication.

To verify that the sudden movement of the couch does not cause unwanted patient motion, the surface guidance detected patient shift after the couch correction was subtracted from the applied couch shift. The mean and standard deviation of the difference were calculated.

All statistical analysis was performed in MATLAB (MathWorks, Natick, MA, USA). Multiway ANOVA was performed to assess the influence of the patient, total fraction time and fraction number on the total baseline drift at the end of the fraction.

3. Results

The median baseline drift and the rate of drift is shown in Fig. 2. The total drift at the end of the fraction was -1.8 ± 1.5 mm in the anterior-posterior (AP), -0.0 ± 1.7 mm in the cranio-caudal (CC) and 0.1 ± 1.8 mm in the medio-lateral (ML) direction. The contribution of baseline drift during the IGRT procedure – image acquisition and evaluation – to the total drift is shown in Fig. 3. In 20% of fractions the patients position displayed non-monotic behavior by returning to the baseline position after the IGRT procedure resulting in a smaller drift at the end of the fraction. For all other fractions the drift during the IGRT procedure was on average 75% of the total drift. In 31% of fractions the maximum baseline drift was over 3 mm and in 3.6% over 5 mm. The peak-to-peak breathing amplitude was smaller than the total baseline drift for 69% of fractions.

The rate of baseline drift was largest between 1 and 2 min after the start of monitoring, namely -0.62 mm/min ($\pm$ 0.68 mm/min) for all patients combined, so generally during image acquisition and evaluation. Baseline drift stabilized after 4 min (rate < 0.2 mm/min) for all
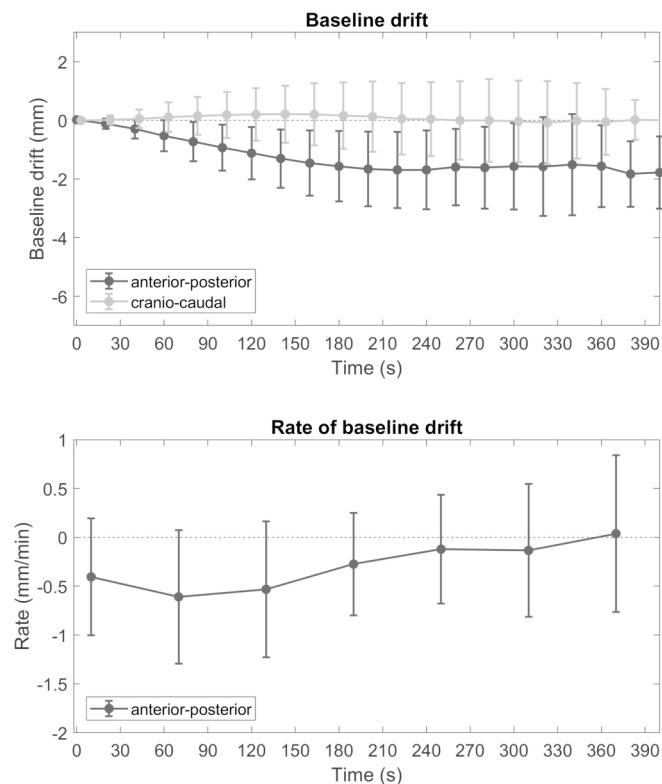

Fig. 2. (top) Median baseline drift for all patients with interquartile range. The cranio-caudal component is offset for visual clarity. (bottom) The mean rate of baseline drift sampled every 60 s. Only the AP component is displayed as the CC component was minimal. Drift is shown up to 400 s due to limited data after this point.

patients combined. Subgroup analysis showed that stability is not reached for breast cancer patients. For breast cancer patients the rate of baseline drift remains above 0.3 mm/min at every point during the fraction. This can partly be attributed to the short overall treatment time. Multi-way ANOVA indicated an impact of the patient and fraction duration on the baseline drift at the end of the fraction ($p < 0.001$). Fraction number had no impact ($p = 0.33$).

The difference between the surface scanning detected couch shift and applied couch shift is shown in Fig. 4. The mean difference was 0.23 mm ($\pm$ 0.7 mm) for all translations and mean 0.1° ($\pm$ 0.2°) for the rotations indicating no major disturbance of the patient due to the sudden couch motion.

4. Discussion

In this study we have monitored patient motion during brief VMAT and IMRT treatment sessions in a fast rotating closed-bore system. In contrast to the majority of published studies we continuously measured patient motion starting at the completion of patient setup while most studies start after initial imaging. Thus we observed that patient baseline drift was largest in the first two minutes, namely during the IGRT procedure. Moreover, the surface scanning system allowed to monitor motion of the entire breast or entire chest wall for lung and esophageal cancer patients providing more information on patient motion compared to studies using a single marker, either a laser focused on the xiphoid process [6], or an infrared marker block placed on the patients' chest [8].

A systematic drift in the posterior direction and negligible drift in the cranio-caudal direction is observed, which is consistent with literature [6,9,22] and believed to be caused by muscle relaxation in the torso and shoulders. The majority of the total baseline drift was observed during the first minutes after initial positioning. 75% of the total drift occured during the IGRT procedure in our study which constituted 60% of the total time patients spent in the treatment position. Jensen et al. [6] similarly detects 90% of the total drift in first 3 min of the fraction for breast cancer patients. Wiant et al. [11] reports stabilization of the patient only after 6–10 min while monitoring free breathing breast cancer patients using surface guidance. In contrast, Hoekstra et al. [10] noted no stabilization for Accelerated Partial Breast Irradiation (APBI) treatments where the mean fraction duration was 26 min. On C-arm linacs volumetric image acquisition requires the extension of the kV-source and imager and rotation of the gantry to the correct starting angle. Additionally, acquisition times can exceed 1 min. C-arm treatment fractions are therefore less affected by initial patient motion during the first 2 min. On the fast rotating closed-bore linac on the other hand, imaging can be initiated within seconds after positioning. It remains unclear how acquiring verification images at this point of transient motion affects the treatment accuracy. The main concern is motion immediately succeeding image acquisition, namely during image evaluation, whereby the patient deviates from the position used for online corrections. Unnoticed (systematic) drift during this time might result in systematic geometrical errors in the delivered dose. In our study drift during the IGRT procedure never exceeded the CTV-to-PTV margin.

Jensen et al. [6] reports different patient behavior during the first fraction for breast cancer patients where close to no baseline drift was observed, compared to subsequent fractions. The authors pose this can be caused by limited muscle relaxation during the first fraction due to patient stress. We did not observe this trend and literature varies. Ricotti et al. [9] also do not observe a correlation between the fraction number and patient drift. Fraction duration however does correlate to baseline drift at the end of the fraction where a longer fraction results in a higher drift, as is observed by Reitz et al. [7], Hoekstra et al. [10] and Wiant et al. [11] for breast cancer patients.

Several authors detect a cranio-caudal drift during a fraction due to the patient slipping from the tilted breast board [6,23]. This effect was not observed in our study as all patients were immobilized at a 0° tilt
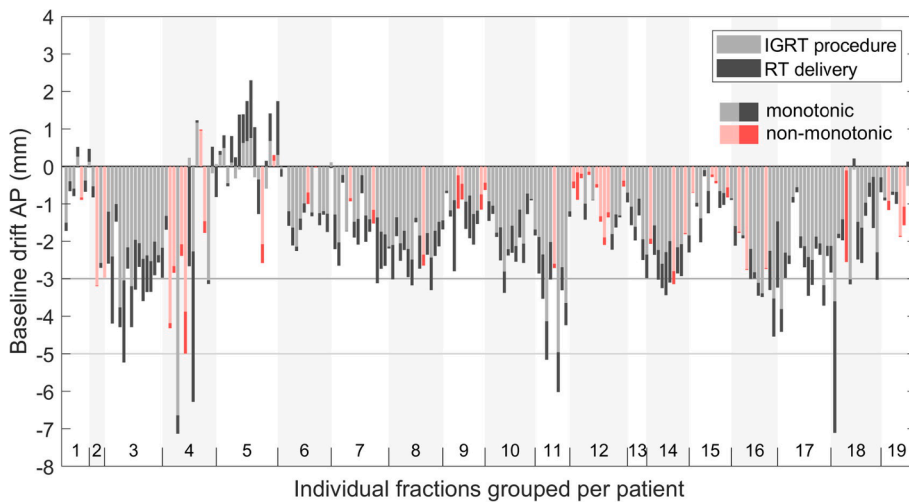
Fig. 3. Total baseline drift in the anterior-posterior direction at the end of the fraction listed per patient. Drift is decomposed in a component of the IGRT procedure (image acquisition and evaluation) and treatment. Fractions in pink indicate that the patient performed a non-monotonic drift and returned closer to the baseline position after the IGRT procedure. The majority of drift occurs during the IGRT procedure compared to treatment delivery and is in the posterior direction. (For interpretation of the references to colour in this figure legend, the reader is referred to the web version of this article.)
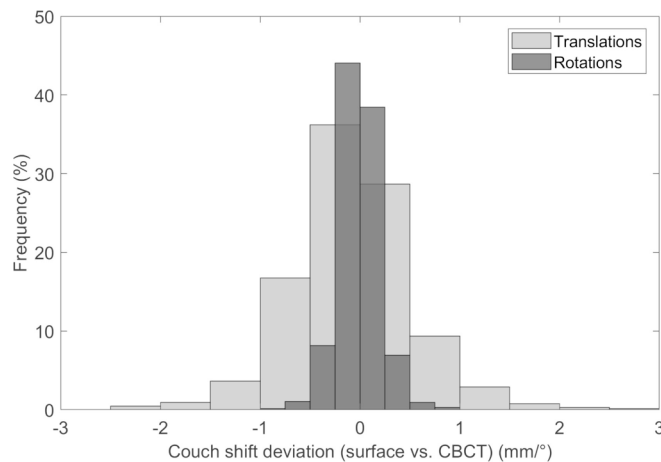
Fig. 4. The difference between the applied couch shift after online position verification of the CBCT and surface detected shift.

where slipping was not expected.

A limitation of our study is that no internal imaging was available during or after treatment. The linac has no option to schedule intermittent imaging. Additional CBCTs mid-fraction e.g. require beam interruptions between automated fields which is not easily implemented. We therefore elected to monitor patients using the standard-of-care. The correlation between external chest motion and the target location for lung and esophageal cancer patients is therefore unclear [24]. Nevertheless, the detection of chest motion indicates patient relaxation or motion and some internal deviations are to be expected.

Another limitation is that the exact timing of several steps are unknown. Initiation of surface imaging after completion of setup was performed by the first author to avoid variability between patients and fractions. The pre-surface imaging relaxation is therefore expected to be negligible. More importantly is that the timing of image acquisition relative to the start of the surface imaging signal is not known. However, RTTs left the treatment room immediately after shifting the patient to the treatment isocenter after which surface imaging was initiated. As the kV-CBCT required maximally 30 s, the entire acquisition was expected to be performed within one minute from the start of the surface imaging signal. As the largest rate of baseline drift was observed from one to two minutes after transfer to the treatment isocenter, the patient continued drifting from their original position during this 'dead time' of volumetric image evaluation as mentioned previously. This is of special interest with the introduction of online adaptive radiotherapy strategies. After

CBCT acquisition Artificial Intelligence (AI) powered contouring of organs-at-risk is performed requiring user-verification after which the plan is re-optimized. These additional steps, which depending on the technology requires up to 20 min [25–27], require the patient to remain motionless during an extended time else any endeavors to adapt the treatment are rendered fruitless. Now, with the release of a commercial online adaptive treatment platform, which has the same closed-bore geometry as the closed-bore linac, we believe in the necessity of continuous patient monitoring prior to, during and after image acquisition in closed-bore gantry systems. Nguyen et al. [21] monitored breast cancer patients using a commercial intra bore surface guidance system during treatment and they detected post-CBCT movement up to 5–7 mm further demonstrating the need for intra-bore monitoring.

Continuous intra-bore optical surface monitoring during imaging and radiation delivery provides valuable information on patient motion during fast VMAT or IMRT treatments in a closed-bore linac. Baseline drift during CBCT acquisition and evaluation during the first minutes after completion of patient setup is not negligible and should be considered during online adaptive workflows.

Declaration of Competing Interest

The authors declare the following financial interests/personal relationships which may be considered as potential competing interests: This work was supported by Varian Medical Systems.

References

[1] van Herk M, Remeijer P, Rasch C, Lebesque JV. The probability of correct target dosage. Int J Radiat Oncol Biol Phys 2000;4:1121–35.

[2] Takao S, Miyamoto N, Matsuura T, Onimaru R, Katoh N, Inoue T, et al. Intrafractional baseline shift or drift of lung tumor motion during gated radiation therapy with a real-time tumor-tracking system. Int J Radiat Oncol Biol Phys 2016; 1:172–80. https://doi.org/10.1016/j.ijrobp.2015.09.024.

[3] Chan MKH, Kwong DLW, Tam E, Tong A, Ng SCY. Quantifying variability of intrafractional target motion in stereotactic body radiotherapy for lung cancers. J Appl Clin Med Phys 2013;5:140–52. https://doi.org/10.1120/jacmp.v14i5.4319.

[4] Worm ES, Høyer M, Fledelius W, Poulsen PR. Three-dimensional, time-resolved, intrafraction motion monitoring throughout stereotactic liver radiation therapy on a conventional linear accelerator. Int J Radiat Oncol Biol Phys 2013;1:190–7. https://doi.org/10.1016/j.ijrobp.2012.12.017.

[5] Dhont J, Vandemeulebroucke J, Burghelea M, Poels K, Depuydt T, Van Den Begin R, et al. The long- and short-term variability of breathing induced tumor motion in lung and liver over the course of a radiotherapy treatment. Radiother Oncol 2017. https://doi.org/10.1016/j.radonc.2017.09.001.

[6] Jensen CA, Acosta Roa AM, Lund JÅ, Frengen J. Intrafractional baseline drift during free breathing breast cancer radiation therapy. Acta Oncol 2017;56(6): 867–73. https://doi.org/10.1080/0284186X.2017.1288924.

[7] Reitz D, Carl G, Schönecker S, Pazos M, Freislederer P, Niyazi M, et al. Real-time intra-fraction motion management in breast cancer radiotherapy. Rad Oncol 2018; 1:128. https://doi.org/10.1186/s13014-018-1072-4.

[8] Quirk S, Becker N, Smith WL. External respiratory motion analysis and statistics for patients and volunteers. J Appl Clin Med Phys 2013;2:4051. https://doi.org/10.1120/jacmp.v14i2.4051.

[9] Ricotti R, Ciardo D, Fattori G, Leonardi MC, Morra A, Dicuonzo S, et al. Intra-fraction respiratory motion and baseline drift during breast Helical Tomotherapy. Radiother Oncol 2017;1:79–86. https://doi.org/10.1016/j.radonc.2016.07.019.

[10] Hoekstra N, Habraken S, Swaak-Kragten A, Hoogeman M, Pignol J-P. Intrafraction motion during partial breast irradiation depends on treatment time. Radiother Oncol 2021;2:73. https://doi.org/10.1016/j.radonc.2021.03.029.

[11] Wiant DB, Wentworth S, Maurer JM, Vanderstraeten CL, Terrell JA, Sintay BJ. Surface imaging-based analysis of intrafraction motion for breast radiotherapy patients. J Appl Clin Med Phys 2014;6:147–59. https://doi.org/10.1120/jacmp.v15i6.4957.

[12] Michiels S, Poels K, Crijns W, Delombaerde L, Roover R, Vanstraelen B, et al. Volumetric modulated arc therapy of head-and-neck cancer on a fast-rotating O-ring linac. Radiother Oncol 2018;3:479–84. https://doi.org/10.1016/j.radonc.2018.04.021.

[13] Barsky AR, O'Grady F, Kennedy C, Taunk NK, Dong L, Metz JM, et al. Initial clinical experience treating patients with breast cancer on a 6-MV flattening-filter-free O-ring linear accelerator. Adv Rad Oncol 2019;4:571–8. https://doi.org/10.1016/j.adro.2019.05.006.

[14] Cozzi L, Fogliata A, Thompson S, Franzese C, Franceschini D, Rose F, et al. Critical appraisal of the treatment planning performance of volumetric modulated arc therapy by means of a dual layer stacked multileaf collimator for head and neck, breast, and prostate. *Technol Cancer Res Treat* 2018:1533033818803882;doi: 10.1177/1533033818803882.

[15] Flores-Martinez E, Cerviño LI, Pawlicki T, Kim GY. Assessment of the use of different imaging and delivery techniques for cranial treatments on the Halcyon linac. J Appl Clin Med Phys 2020. https://doi.org/10.1002/acm2.12772.

[16] Delombaerde L, Petillion S, Weltens C, Depuydt T. Spirometer-guided breath-hold breast VMAT verified with portal images and surface tracking. Radiother Oncol 2021;157:78–84. https://doi.org/10.1016/j.radonc.2021.01.016.

[17] Nguyen D, Farah J, Josserand-Pietri F, Barbet N, Khodri M. Benefits and challenges of standard ceiling-mounted surface guided radiotherapy systems for breast treatments on Halcyon™. Radioprotection 2021;6:e235.

[18] Delombaerde L, Petillion S, Depuydt T. EP-2051: Surface scanner camera position optimization on the Varian Halcyon TM O-ring gantry linac system. *Radiother Oncol* 2018:S1122–S1123.

[19] Delombaerde L, Petillion S, Michiels S, Weltens C, Depuydt T. Development and accuracy evaluation of a single-camera intra-bore surface scanning system for radiotherapy in an O-ring linac. Phys Imaging Radiat Oncol 2019;21–6. https://doi.org/10.1016/j.phro.2019.07.003.

[20] Nguyen D, Farah J, Barbet N, Khodri M. Commissioning and performance testing of the first prototype of AlignRT InBore™ a Halcyon™ and Ethos™-dedicated surface guided radiation therapy platform. Phys Med 2020:159–66. https://doi.org/10.1016/j.ejmp.2020.10.024.

[21] Nguyen D, Yossi S, Lorchel F, Pouchard I, Renoult F, Barbet N, et al. Reporting the first clinical implementation of Alignrt Inbore, the New Halcyon™-dedicated surface guided radiation therapy solution. Int J Radiat Oncol Biol Phys 2020;108: e319. https://doi.org/10.1016/j.ijrobp.2020.07.762.

[22] Hirata K, Yoshimura M, Mukumoto N, Nakamura M, Inoue M, Sasaki M, et al. Three-dimensional intrafractional internal target motions in accelerated partial breast irradiation using three-dimensional conformal external beam radiotherapy. Radiother Oncol 2017;1:118–23. https://doi.org/10.1016/j.radonc.2017.04.023.

[23] Crop F, Pasquier D, Baczkiewic A, Doré J, Bequet L, Steux E, et al. Surface imaging, laser positioning or volumetric imaging for breast cancer with nodal involvement treated by helical TomoTherapy. J Appl Clin Med Phys 2016;5:200–11. https://doi.org/10.1120/jacmp.v17i5.6041.

[24] Hoisak JDP, Sixel KE, Tirona R, Cheung PCF, Pignol JP. Correlation of lung tumor motion with external surrogate indicators of respiration. Int J Radiat Oncol Biol Phys 2004;4:1298–306. https://doi.org/10.1016/j.ijrobp.2004.07.681.

[25] Raaymakers BW, Jürgenliemk-Schulz IM, Bol GH, Glitzner M, Kotte ANTJ, van Asselen B, et al. First patients treated with a 1.5 T MRI-Linac. Phys Med Biol 2017; 23:L41–50. https://doi.org/10.1088/1361-6560/aa9517.

[26] Green OL, Henke LE, Hugo GD. Practical clinical workflows for online and offline adaptive radiation therapy. Sem Rad Oncol 2019;3:219–27. https://doi.org/10.1016/j.semradonc.2019.02.004.

[27] Yoon SW, Lin H, Alonso-Basanta M, Anderson N, Apinorasethkul O, Cooper K, et al. Initial evaluation of a novel cone-beam CT-based semi-automated online adaptive radiotherapy system for head and neck cancer treatment – A timing and automation quality study. *Cureus* 2020;8:e9660;doi:10.7759/cureus.9660.